

Geological Society, London, Special Publications

Flexure and 'unflexure' of the North Alpine German-Austrian Molasse Basin: constraints from forward tectonic modelling

B. Andeweg and S. Cloetingh

Geological Society, London, Special Publications 1998; v. 134; p. 403-422
doi:10.1144/GSL.SP.1998.134.01.19

Email alerting service [click here](#) to receive free email alerts when new articles cite this article

Permission request [click here](#) to seek permission to re-use all or part of this article

Subscribe [click here](#) to subscribe to Geological Society, London, Special Publications or the Lyell Collection

Notes

Downloaded by Vrije Universiteit on 6 March 2009

Flexure and 'unflexure' of the North Alpine German–Austrian Molasse Basin: constraints from forward tectonic modelling

B. ANDEWEG & S. CLOETINGH

Faculty of Earth Sciences, Vrije Universiteit, De Boelelaan 1085, 1081 HV Amsterdam.

Abstract: We present the results of forward modelling of the Northern Alpine German–Austrian Molasse Basin, which forms part of the Northern Alpine Foreland Basin (NAFB) extending from Lake Geneva in the west to Lower Austria in the east. The observed deflection of the European plate under the NAFB has been modelled along five profiles perpendicular to the basin axis. Models treating the deflection of the NAFB as a flexural response to loading only, require a set of loading parameters (bending moment, vertical force) which would imply bending stresses exceeding the strength of the subsiding plate. Moreover, this approach would not take into account the significant post-Molasse uplift experienced by the Alpine chain and its northern foreland basins. We modelled the deflection as the response to two distinct processes: (1) flexure of an elastic plate with lateral variations (EET-values of 7–26 km from east to west) loaded with surface and limited subsurface loads and (2) the Late Cenozoic (post-molasse) phase of 'unflexing', significant uplift observed in the Alps and its northern foreland. Our study provides a first attempt to separate these two processes in order to model the deflection by an elastic plate-model, adopting flexural parameters that will not exceed the strength of the lithosphere.

The Alpine mountain chain is a classic continent-continent collision zone. During its evolution the African continental plate overthrust the European margin and stacked slices of the European plate on to the European plate. This acted as a (topographic) load translating over the underthrusting plate. Due to this loading a flexural deflection developed in front of the thrust belt. As a result of the in general low flexural rigidity of the downgoing lithosphere this led to a deep and narrow basin, just as the Ebro (Zoetemeijer *et al.* 1990; Millan *et al.* 1995), Apennine (Royden 1993; Kruse & Royden 1994), Carpathian (Matenco *et al.* 1997) and Swiss Molasse basins (Sinclair *et al.* 1991). The Northern Alpine Foreland Basin (NAFB, see Fig. 1) is considered to be a classical example of this type of basins, featuring a strongly asymmetrical geometry, deepening towards the Alpine mountain front and present along all of the northern part of the Alps and the Carpathians. Although its overall shape appears to be primarily the result of the emplacement of the Alpine nappes, remarkable lateral variations in geometry and kinematics of the NAFB can be observed that distort the simple theoretic asymmetrical shape. The Basin is developed or preserved best in its German part where it is 150 km wide and contains a sedimentary infill of upto almost 5000m (Lemcke 1988; Bachmann & Muller 1992). To the east, in direction of Austria, the Basin narrows to only 15 km and becomes shallower where the crystalline Bohemian Massif is close to the frontal thrusts of the Alps

and broadens again to the Carpathian foreland. To the west, in Switzerland, the Basin narrows as well, probably related to the considerable Cenozoic uplift of up to 2500 m (Lemcke 1988) that has destroyed part of its original extent. In this respect it might not be coincidence that this highly uplifted part is situated at the southern termination of the Rhine Graben (Gutscher 1995) and related to local uplift leading to the Jura Mountains. These lateral variations from Switzerland to Austria are probably the product of a combination of processes such as variations in strength of the downgoing European lithosphere, pre-subsidence geological setting, lateral inhomogeneties of the basement (basement faults) and recent significant laterally varying uplift.

Modelling the flexure of the European plate underlying the NAFB has been the subject of several studies over the last decades. Most of the authors conclude that the geometry of the NAFB, the asymmetric flexural depression that developed in front of migrating thrust loads of the Alps, can be modelled by an elastic plate overlying an inviscous fluid loaded by the orogenic thrust wedge. The resultant values for the effective elastic thickness of the downflexing European plate show, however, a very wide range: from 35–50 km to only 7.5 km. A source of controversy between most of the studies is the concept of additional subsurface loads; applying a bending moment (M_0) and/or a vertical shear forces (V_0) at the free end of the plate to enhance deflection. In order to simulate the

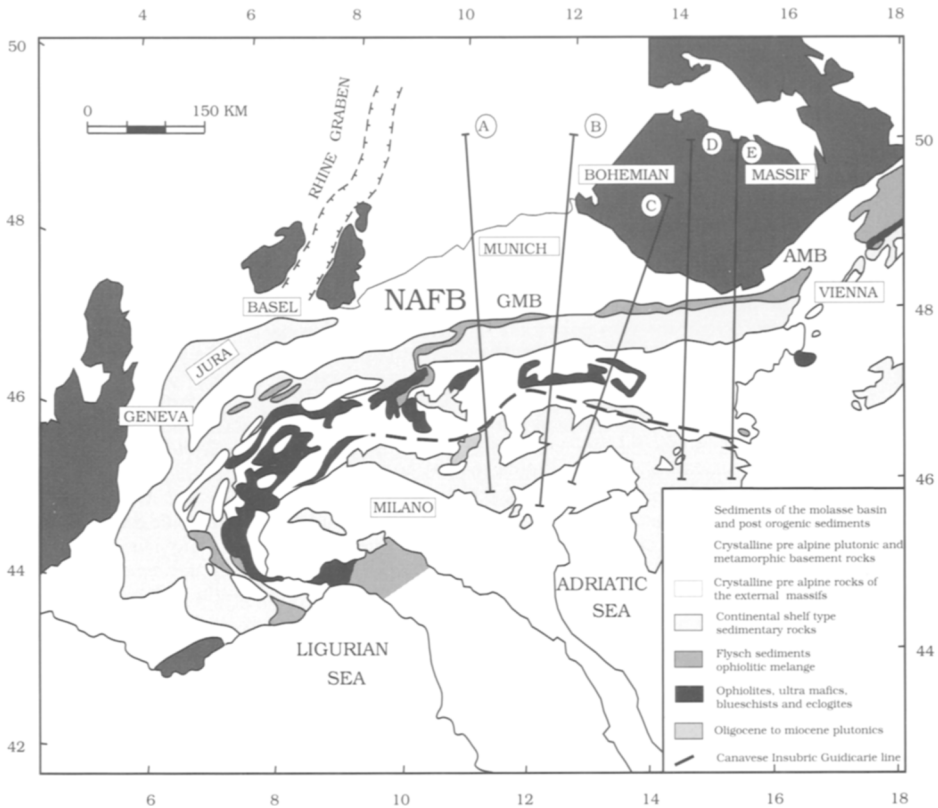


Fig. 1. General setting of the Alpine mountain chain showing the arcuate couple of thrust belt and foreland basin and different tectono-sedimentary areas. Location of the Northern Alpine Foreland Basin (NAFB), the German Molasse Basin (GMB), the Austrian Molasse Basin (AMB) and the five modelled profiles (A–E) is indicated.

observed deflection many authors make unlimited use of these subsurface loads. To obtain better constraints on the flexural parameters, gravity data have been incorporated in the modelling as an independent constraint.

In the Swiss Molasse Basin both stratigraphy (Sinclair *et al.* 1991; Allen *et al.* 1991), and flexure (Lyon-Caen & Molnar 1989) have been modelled. In contrast, previous work in the German Molasse Basin (GMB) has focused almost entirely on very detailed sedimentological and stratigraphical work, with the aim of correlating the different lithostratigraphic levels of the western and eastern part of the GMB (Bachmann & Müller 1992; Bachmann *et al.* 1987). Some limited modelling of the observed gravity anomalies over the NAFB has been carried out by Karner & Watts (1983) and Royden (1993). The latter author also performed a flexural study. More recently, sequence-stratigraphic patterns combined with flexure of the GMB

have been modelled on a short section through the basin east of Munich by Jin (1995).

The NAFB, the depression of the European lithosphere at the northern side of the Alpine chain, initially is the flexural response of this plate due to loading by overthrusting of the African plate and emplacement of the Alpine nappes. The basin has been filled with Molasse sediments related to the ongoing subsidence. After this deposition, the Alpine chain and its surroundings recently (from Miocene times on) have experienced significant uplift (Lemcke 1988; Jouanne *et al.* 1995; Genser *et al.* 1996, 1997). These two distinct periods in the evolution of the GMB give rise to a very particular geometry: a flexural asymmetric foreland basin that has experienced differential uplift together with the Alpine thrust belt that caused the deflection. Therefore, it seems obvious that it is impossible to model the presently observed geometry of the NAFB by a bending elastic plate

only: (too) large subsurface loads would be required to account for the tight curvature. In this paper we investigate whether the elastic plate model can adequately explain the observed geometry if the two processes are being separated. Using uplift data to restore the pre-uplift situation and well-log, deep seismic and gravity data, the observed geometry along five profiles through the NAFB has been modelled.

Stratigraphy of the Northern Alpine Molasse Basin

The NAFB is filled with (at the present Alpine thrust front) up to 5000 m predominantly clastic sediments of Tertiary age. The base of this so-called Molasse lapped progressively northwards on to a peneplained differentiated basement consisting of Mesozoic shelf sediments, local Permo-Carboniferous graben sediments and Variscan basement. Seismic and well data show that the southward-dipping sediments continue underneath the Alpine nappes to at least 50 km (Lemcke 1988).

The stratigraphy of the NAFB is not uniform laterally and major lithostratigraphical differences occur between the western and eastern part of the Basin (see Fig. 2). In the eastern part, more or less marine environments prevailed throughout history, and the western part has been submerged frequently. Jin (1995) distinguished in the area east from Munich three shallowing-upward sequences. In the Swiss foreland basin, classically only two shallowing-up sequences have been described (e.g. Allen *et al.* 1991). For the western part of the GMB, the latter subdivision is more useful. The described transgressions or regressions are due to relative sea-level changes, which can be the consequence of different processes (including intra-plate stress fluctuations, change of sediment input causing over- or underfilling of the basin, eustatic sea-level changes, see e.g. Peper *et al.* 1994).

Sedimentation in the GMB started in the Priabonian (Late Eocene) due to a world-wide rise of sea level (Bachmann & Müller 1992). In an eastward-shallowing and broadening (deep) sea trough, with an axis approximately 50 km south from the present Alpine thrust front, sedimentation of flysch occurred in turbiditic sequences, of up to 650 m ('Deutenhausener Schichten') in the centre of the trough. In the Austrian Molasse Basin (AMB) fluvio-lacustrine sediments were deposited in the north and limestones and marls on the deeper shelf to the southwest (Nachtmann & Wagner 1986).

The flysch sediments (North Helvetic Flysch) are found as allochthonous remnants in the

Folded Molasse, north from the original sedimentation-trough. The flysch is pinching out rapidly in northeastern direction, where a thin cover of Basal Sandstones (20–70 m) and Lithothamnium Limestone (0–100 m) is sedimented as transgression continues over the at least 30 Ma peneplained basement of Cretaceous and karsted Malm. These sediments can be considered to be the first *sensu strictu* Molasse sediments (Lemcke 1988). In the northeastern part of the GMB and the north of the AMB sedimentation of erosion products of the Bohemian Massif is significant (Nachtmann & Wagner 1986). In this area the rate of subsidence (Lemcke 1988) was most of the time kept up by the sedimentation, enabling continental conditions to prevail throughout the development of the basin.

During Rupelian, the sea transgressed more to the north, the basin subsided very rapidly in the southeastern part, where the Rupelian sediments reach a thickness of more than 1200 m. To the west the basin is less deep and less broad: the Lower Marine Molasse (German: UMM), which consists of deeper water (palaeobathymetry: 100–200 m) marls, is near Lake Constance only some 100 m thick and pinches out not far northwards (Bachmann & Müller 1992).

At the Rupelian–Chattian boundary a most likely eustatic induced regression makes the shoreline to shift approximately 150 km to the east, to the Freising–Munich–Miesbach line, where it will remain until the early Late Aquitanian (Eggenburgian). This regression is supposed to be induced by the largest sea-level change since the Cambrian because basin subsidence continues at the same rate and no additional sediment input is observed that would be able to drown the basin. During this regression the Baustein beds, sandbodies derived from the area where the present Folded Molasse is situated and Eastern Switzerland (Lemcke 1988), are deposited.

In the Chattian (Early Egerian) deposition of the Lower Freshwater Molasse (German: USM) occurs in the WGMB. Large river systems, that ran nearly parallel to the mountain chain to the sea in the east (Lemcke 1988), deposited large amounts of sand and silt (LFM 1). In the EGMB and the AMB, marine conditions prevailed, enabling the sedimentation of vast sheets of dark marls (Upper Chattian and Lower Aquitanian Marls). The marls transgressed (moderate sea-level rise and/or decrease in subsidence) at the Chattian–Aquitanian boundary over the Chattian Sands, but regressed again during Aquitanian (Late Egerian) due to a renewed cycle of the Lower Freshwater Molasse (LFM 2).

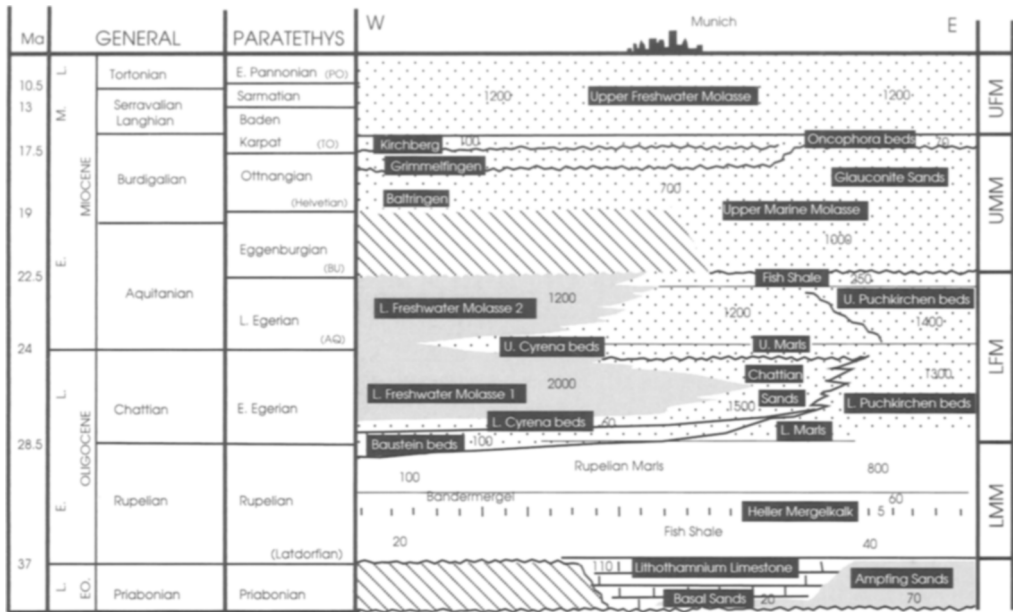


Fig. 2. Schematic west-east stratigraphic section through the NAFB showing generalized sedimentary infill. Note the earlier onset of sedimentation in the eastern part of the basin and the lateral variations in thickness and sediment-type. Modified from Bachmann & Müller (1992).

The top of the Aquitanian became eroded before a second large transgression took place at the beginning of the Burdigalian (Eggenburgian), invoking renewed marl-deposition in the EGMB (Upper Marine Molasse). The ongoing transgression, which reached its peak during the Mid-Burdigalian (Ottngian) and flooded the entire GMB, caused deposition of marls in the WGMB as well (Jin 1995) during Mid-Burdigalian (Ottngian, German: OMM).

The marine basin became filled during Late Burdigalian (Late Ottngian-Karpatian) and until the Tortonian (Late Pannonian), in the entire basin the Upper Freshwater Molasse (German: OSM) was deposited. This again took place parallel to the axis of the basin. This time, however, the sediment sources were situated in the western part of the Austrian Molasse Basin, so sediment transport occurred from east to west. This UFM marks the end of the flexure related sedimentation in the NAFB.

Flexural modelling

Modelling strategy

The flexural response of the European lithosphere to loading by the thrust sheets of the Alps has been studied along five profiles through this

orogen and its northern Molasse Basin (for location profiles see Fig. 1). These profiles are taken more or less perpendicular to the axis of the basin. The observed deflection and gravity data were used to constrain the flexural parameters by forward modelling the deflection using a two-dimensional finite-difference technique (Bodine *et al.* 1981), which allows the incorporation of lateral variations in mechanical properties and distributed loads. For a broken-plate model, the deflection of an elastic plate under a given topographic load is calculated interactively, incorporating (secondary) loading by infill of the created space with material of a specified density. Variation of density with depth is not possible, so an average has been taken for the sedimentary infill. Additional subsurface loads (vertical shear forces, V_0 and bending moments, M_0 at the free end of the plate or horizontal stresses) can be incorporated (see Fig. 3). Finite-difference calculations have been performed along 2000 km long profiles to minimize end effects. Additionally, the gravity anomaly that would result from the flexural model is calculated. The infill of the flexural depression as well as the effect of the subsurface loads is taken into account in this gravity calculation.

The gravity data were kindly placed at our disposal by the ÖMV, density data of crust, mantle

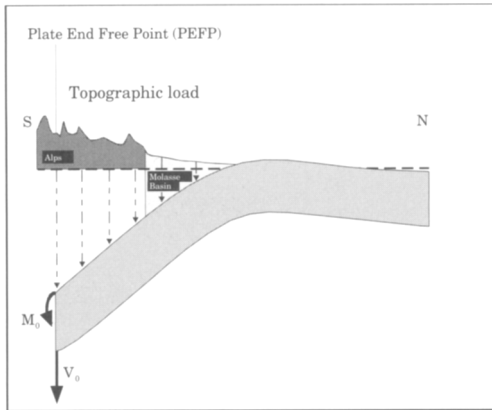


Fig. 3. Schematic illustration showing the modelling configuration. Loading due to a combination of topographic loading and additional subsurface forces applied to the free end of the overthrust plate. V_o = vertical shear force, M_o = bending moment. Plate end free point (PEFP) is indicated.

and sediments (see Table 1) were taken from Gutscher (1995). Sedimentation of the Basal and Ampfing Sandstones (see Fig. 2) in the eastern GMB over the differentiated Mesozoic basement indicate the onset of flexure in Priabonian (Late Eocene). In the western part of the basin sedimentation related to the deflection of the European plate started in Early Oligocene with deposition of the Fish Shale of the Lower Marine Molasse. We, therefore, have taken the base of the Tertiary as the base of sedimentation in the NAFB related to the overthrusting of the Adriatic–African Plate, a process that started in Late Eocene times. Constraints on the observed depth of the base of the Molasse Basin are derived from well-logs and reflection seismic lines (Lemcke 1988, fig. 54) in the GMB (see Fig. 4). Subsidence of the basin continued until the Late Miocene (Jin 1995; Lemcke 1988), deposition of the Upper Freshwater Molasse marking the end of the Molasse sediments *s.l.*, whereas subsidence ceased during the Mid-Burdigalian (Ottangian c. 19–17.5 Ma) times in the Austrian part of the basin.

After this subsidence, the NAFB experienced a relative stable stage and from Late Pannonian

(c. 7.1 Ma) uplift of several hundreds of metres (Genser *et al.* 1996). Data used in this work are derived from quantitative subsidence analysis of a number of wells (Genser pers. comm.) for the Austrian part and from Lemcke (1988) for the German part of the basin (see Fig. 5). These data are in agreement with the recent uplift data obtained by geophysical and geodetic methods in the Central Alps (Trümpy 1980, Fig. 43) and the northwestern Alps, the Molasse basin and the southern Jura mountains (Jouanne *et al.* 1995). This uplift of up to 730 m suggests that the basin extended much further northwards during deposition of the Molasse than the present erosional edge. This edge is observed at nearly 700 m height in the eastern and at 400 m in the western part of the GMB whereas the sediments were deposited at approximately 50–100 m (Lemcke 1988). Although we realized that locally small scale tectonics might have added to the uplift (for example the development of the Jura Mountains), we have not been able to develop a separate database for a general uplift and local effects. Whenever the uplift database becomes more detailed, this should be taken into account.

We have restored the pre-uplift situation, subtracting the Cenozoic uplift values from the observed present basement depth and modelled this reconstructed palaeo-deflection. The fit to the present deflection can be obtained from the inferred palaeo-deflection plus the observed Cenozoic uplift. This will change the predicted gravity anomaly by:

$$\Delta g = 2\pi\Delta\rho Gw_{(x)}. \quad (\text{Eq. 1})$$

For $G = 6.67 \times 10^{-11} \text{ Nm}^2 \text{ kg}^{-2}$ and a density difference between mantle and infill ($\rho_m - \rho_i$) of 800 kg m^{-3} , this difference in the anomaly will be -3.3527 mGal for every 100 m uplift. This is only correct if the uplift is relatively small, the contribution to the gravity anomaly of a density-difference decreases with increasing depth. Moreover, the origin of the ‘unflexing’ can have adjusted the anomaly significantly (dependent on how the volume increase due to the uplift is treated: density decrease versus input of mantle-material). We assumed the crustal thickness to remain constant during uplift. This seems to be

Table 1. Densities used in the forward modelling (taken from Gutscher 1995)

Materials	Density (km m^{-3}) used
Sediments	2450–2550
Load	2550–2670
Crust	2720–2900
Mantle	3200–3300

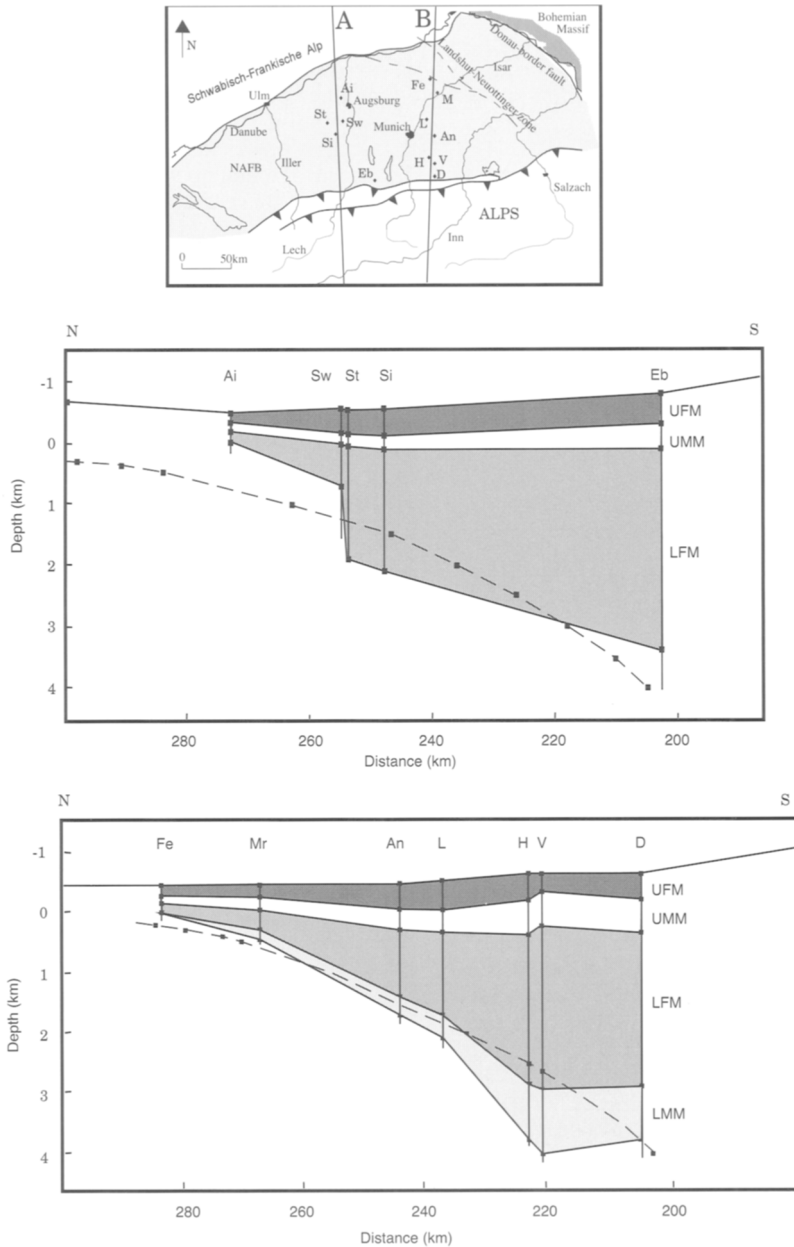


Fig. 4. Observations of the several stages (LMM, Lower Marine Molasse; LFM, Lower Freshwater Molasse; UMM, Upper Marine Molasse; UFM, Upper Freshwater Molasse) of the Molasse sediments in the NAFB. **Upper panel:** location of profiles A and B and deep drilling wells (Ai, Aichach 1001; Sw, Schwabmünchen 1; St, Scherstetten 1; Si, Siebnach 1, Eb (projected), Eberfing 1; Fe, Freising 1003; M, Moosburg 1; L, Landsham 1; An, Anzing 3; H, Holzkirchen 1; V, Vagen; and D, Darching 1). **Middle panel:** depth observations of the several Molasse stages for profile A. Dashed line shows shape of the basin used in the modelling (modified after Lemcke 1988, using seismics but neglecting local deformation). Position of the wells is given in respect to the origin of the profile lines. **Lower panel:** profile B, figure convention as in middle panel.

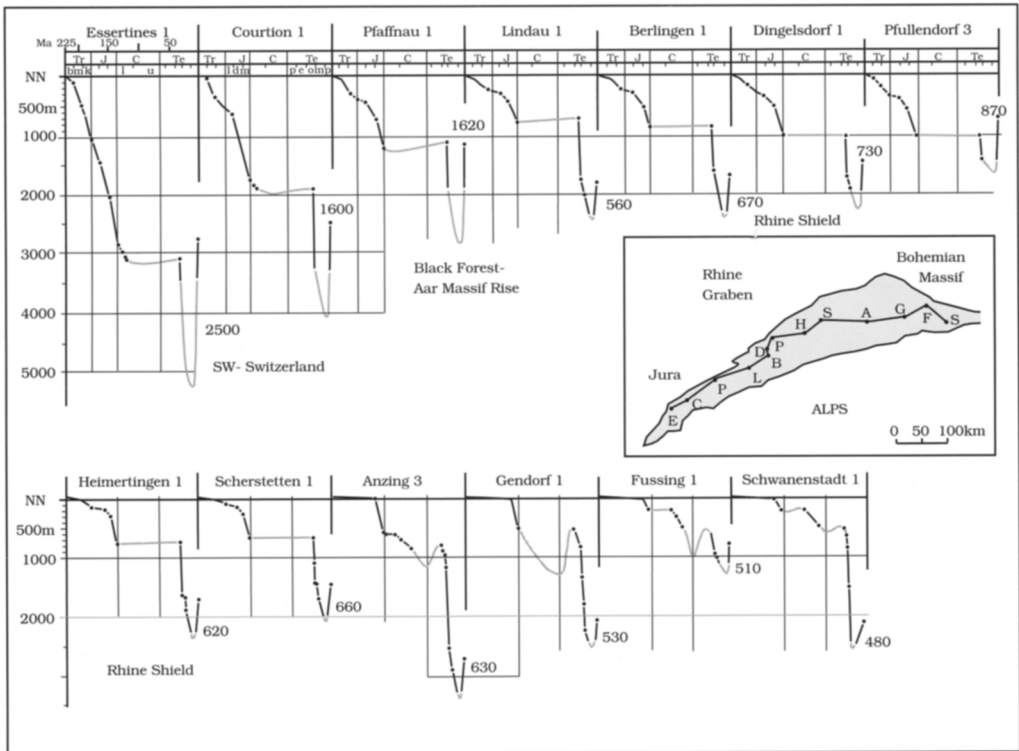


Fig. 5. Subsidence curves of several wells showing the significant Late Cenozoic uplift of the German part of the NAFB. Grey lines denote eroded parts of the stratigraphy. Inset figure shows position of the wells. Uplift values in numbers along the curves. Tr, Triassic (subdivision b, Buntsandstein; m, Muschelkalk; k, Keuper); J, Jurassic (l, Lias; d, Dogger; m, Malm); C, Cretaceous (l, Lower; u, Upper); Te, Tertiary (p, Paleogene; e, Eocene; o, Oligocene; m, Miocene; p, Pliocene). Notice the lateral variation and the general decrease of the uplift from west to east (after Lemcke 1974).

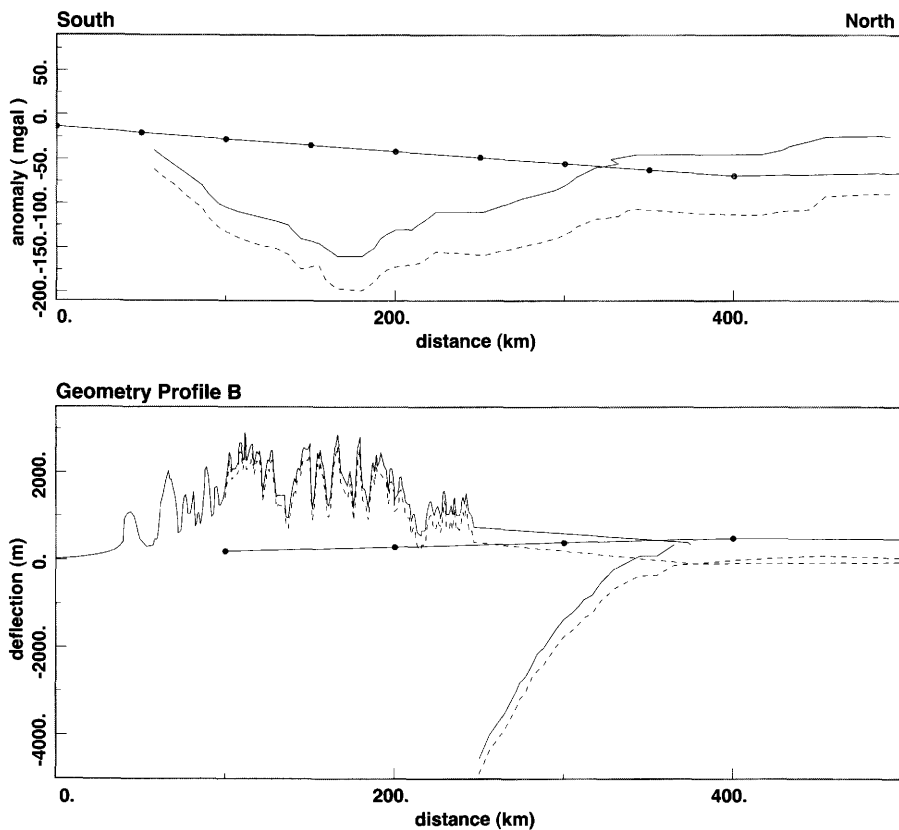
justified because during the small timespan (c.5 Ma) of the uplift, the crustal thickness would not increase (by thermal aging) or decrease significantly. Combined with the uplift profile, used to restore the pre-uplift geometry, the pre-uplift situation has been modelled. This approach provides only a first-order estimate as the uplift database of the basin is far from complete and not much is known about palaeo-topography of the Alps. There are some ideas concerning palaeo-topography, but since equation 1 is only valid for cylindrical topography, more accuracy is not needed. After the most important thrust events during Tertiary times, at least part of the mountain chain has been uplifted. It is not the prime aim of this study to derive a detailed estimate of the palaeo-topography or 'palaeo-gravity anomalies' of the Alps. Here we illustrate only the concept of treating the present geometry of the NAFB as the result of a flexural deflection of the European plate subsequently modified by

recent uplift of several hundreds of metres.

In this way, the pre-uplift situation has been restored for all of the profiles (see Fig. 6 for profile B). Using flexure modelling software (Zoetemeijer 1993), the deflection of the European Plate was modelled. Free parameters were: EET, Plate end free point (PEFP), V_0 and M_0 . The outcome is not an unique solution, but the combination of the four free parameters confine the range of possibilities and narrow down adequately the range of possible solutions.

Subsurface loads

To obtain the deflection of the lithosphere underlying the NAFB, topographic loading alone is not sufficient. This situation is similar to the Carpathians and Apennine foreland basins, requiring additional subsurface loads (Royden & Karner 1984). With these loads acting on the foreland lithosphere that are not expressed as



Present observations and the pre-uplift situation

Fig. 6. Approach to restore the pre-uplift situation for Profile B. **Upper panel:** observed Bouguer anomaly (solid line), anomaly difference resulting from uplift (solid line with dots) and pre-uplift anomaly (dashed line). **Lower panel:** present-day topography (solid line), uplift profile (solid line with dots) and pre-uplift (uplift subtracted from present-day topography) geometry (dashed line).

surface topography (see Fig. 3), it appears to be possible to reproduce the deflection. The nature of these subsurface loads, however, is not known. Various explanations have been proposed over the last decade: density variations at subcrustal levels (Karner & Watts 1983) caused by a dense subducted slab at subcrustal depths (Royden 1993), transmitted horizontal compression generated by the interaction of plates and their boundaries (Karner & Watts 1983) or dynamic stresses related to subduction (Royden 1993) or downgoing convective flows beneath the lithosphere (Burov & Diament 1995), pre-orogenic structure (Stockmal *et al.* 1987), emplacement of ultramafic bodies onto the downflexing plate (Royden 1993), overthrusting of a deep water continental margin (Royden 1993) or crustal thinning associated with

back-arc rifting processes during active subduction (Karner & Watts 1983). This latter can exist only if the subduction rate is faster than the convergence rate, which in the Alps was most likely not the case.

However, some of the above-mentioned processes have taken place or are observed in the northern Alpine region. It is not possible to reproduce the tight curvature of the European plate by surface-loading by the Alpine chain only. Moreover, when applying subsurface loads taking into account their limits, the deflection of the NAFB can be fitted for every profile. The plate-boundary loads can create significant local strength variations in the bending lithosphere (Burov & Diament 1995). In many of the previous works the subsurface loads were used without limits, probably even much larger than

Table 2. Values of the flexural parameters used for profile 5b abb in Royden (1993)

Parameter	E Alps
EET (km)	40
D (Nm)	4.6×10^{23}
M_o used ($N m^{-1}$)	2.5×10^{17}
w_{max} (m)	6200
α (km)	127.97
M_{max} ($N m^{-1}$)	1.12×10^{17}
W Alps	
EET (km)	50
D (Nm)	9×10^{23}
M_o used ($N m^{-1}$)	9.0×10^{17}
w_{max} (m)	14000
α (km)	151.35
M_{max} ($N m^{-1}$)	3.54×10^{17}

Upper part: taken from Royden (1993, table 2), w_{max} estimated from Royden (1993 figs 9 & 10). Lower part: numerically calculated values. The bending moment used exceeds by far the value that can be supported by the plate.

can be supported by an elastic plate under the used conditions. We made an estimate of the maximum bending moment that can be supported. This estimate (see Appendix) is based on rheological laws and data confining yield-stress envelopes (e.g. Burov & Diament 1995) and analytical solutions of a simple deflection model (Turcotte & Schubert 1982). The lithosphere that is used in the estimate is homogeneous and undeformed. As the lithospheric plate under the NAFB is far from homogeneous and undeformed upon onset of loading, the maximum applicable values for the subsurface loads will therefore be smaller than the theoretical determined values. Therefore, the calculated values can at least be used as an upper limit for the values of the subsurface loads. As an illustration Table 2 shows the flexural parameters that were used by Royden (1993) for forward

modelling the deflection of the European plate along profiles through the Alps and its northern foreland. Using the equations (see Appendix), the maximum bending moment has been determined analytically and is displayed in the tables as well. Inspection of Table 2 shows that if these values would be applied, the elastic strength of the downgoing plate would be exceeded in these cases and, at least part of, the plate would deform plastically or break up.

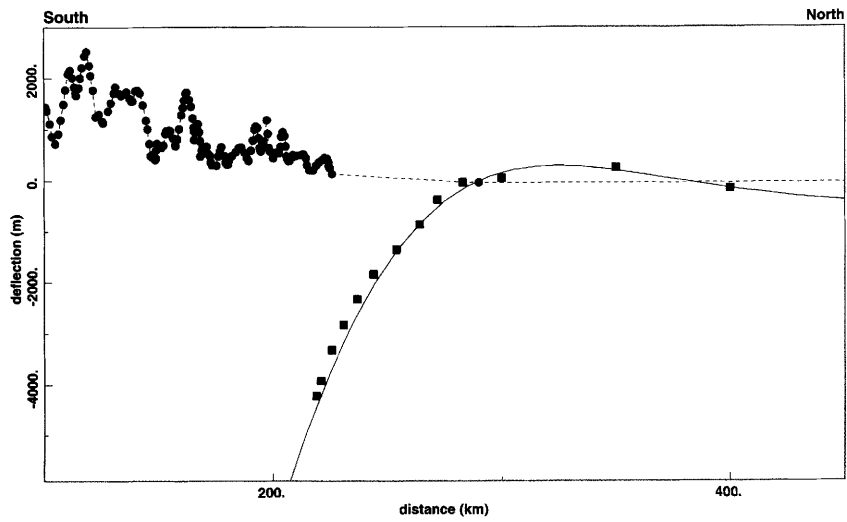
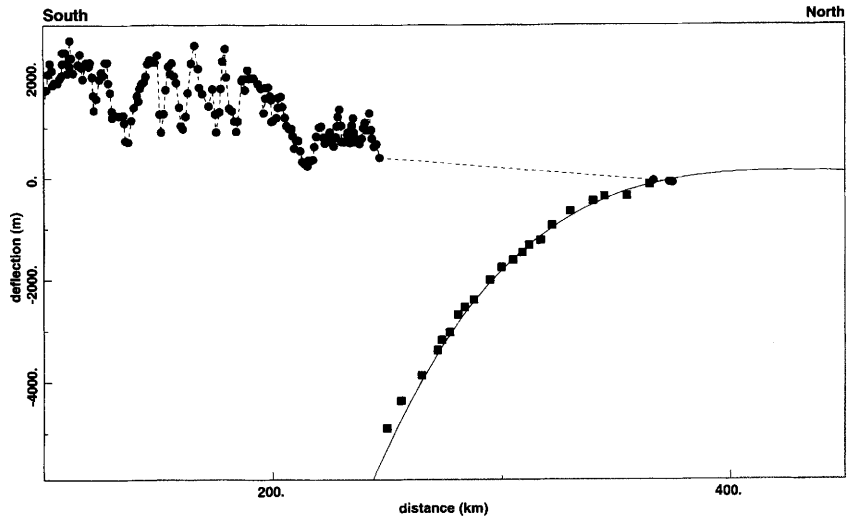
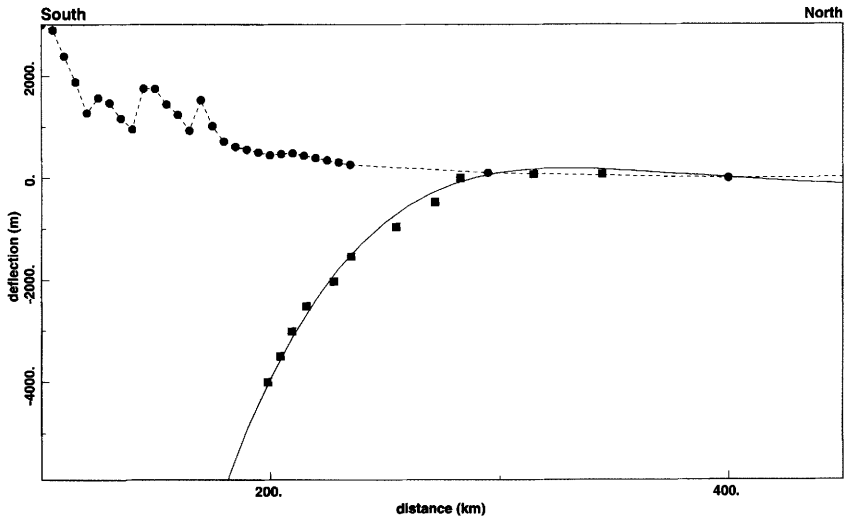
Results

To model the observed deflection along the chosen profiles through the NAFB, without taking into account the recent uplift, requires a set of parameters incompatible with the limits of the strength of the elastic plate and the maximum values of the subsurface loads (see

Table 3. Values of the flexural parameters that would be required to obtain the observed deflection along profile B without taking into account the Late Cenozoic uplift

Parameter	
EET (km)	26
D (Nm)	1.09×10^{23}
M_o used ($N m^{-1}$)	1.7×10^{17}
w_{max} (m)	12542
α (km)	90.58
M_{max} ($N m^{-1}$)	1.08×10^{17}

As can be observed, the bending moment used would exceed the value that can be supported by the plate.



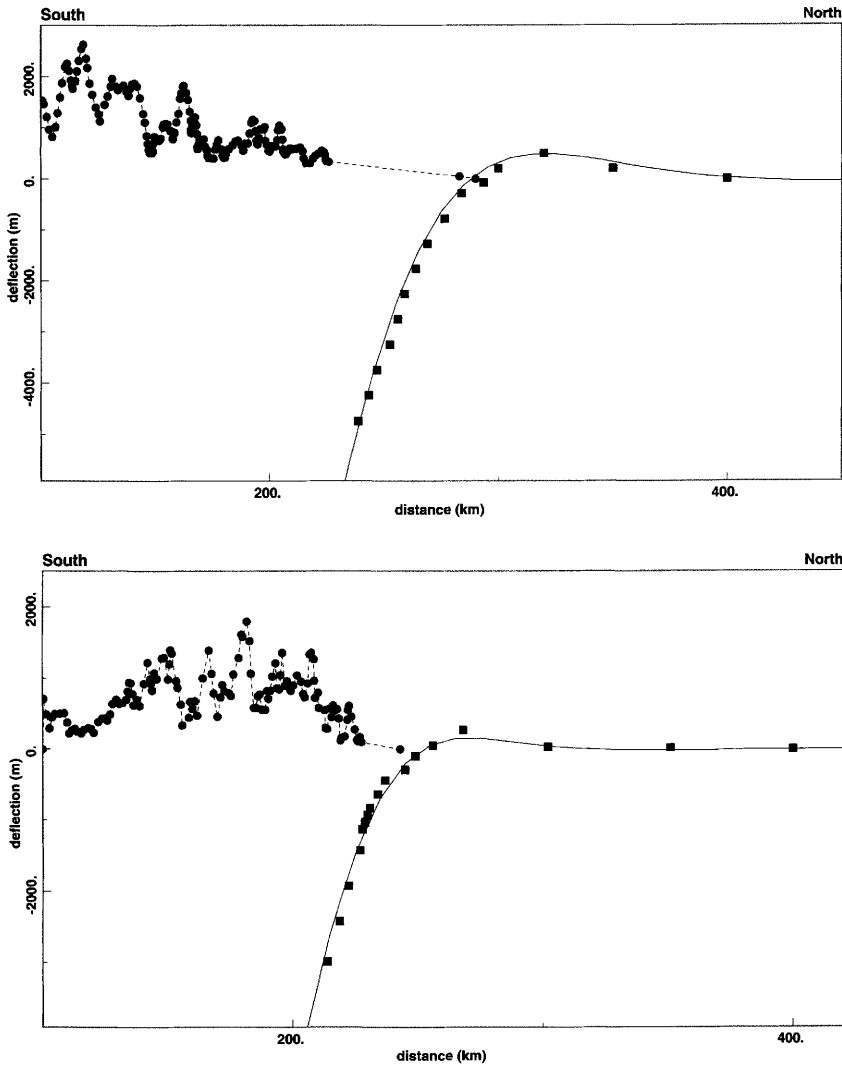


Fig. 7. Best fit for the profiles (A–E) showing topography (dashed line), basement depth data (squares) and the modelled deflection (solid line). For densities used see Table 1, for values of the parameters see Table 4.

Appendix). In Table 3 the parameters that would be needed for profile B are shown, obviously the applied bending moment is too large and as for profile B, the M_0 values used would exceed M_{\max} in all of the profiles.

Following the approach of subtracting the Late Cenozoic uplift from the present topography and using this pre-uplift setting to model the deflection, yields results that for the subsurface loading appear to be much more realistic. Sub-surface loads that are applied are only a fraction of the maximally applicable values. The best fits for the profiles are summarized in Table 4 (for location of the profiles see Fig. 1).

Profile A (Fig. 7a). This profile is close to the location of the European Geotraverse (1992). The best fit is obtained by adopting an EET value of 25 km, a value that is somewhat higher than was suggested by Cloetingh & Banda (1992) on the base of rheological models combined with seismicity cut-offs. The topographic load is largest for profile A, not only due to high topography in the Alps, but also due to the fact that the plate continues far south underneath it (PEFP:100 km from the origin of the profile, see Fig. 8). When V_0 is subtracted from the numerically determined V_{\max} , the load of the Alps results to be $0.93 \times 10^{13} \text{ N m}^{-1}$, a value that is two

Table 4. Table showing values for parameters used to obtain best fits and numerically determined maximum values

Profile	EET (km)	W_0 (m)	W_0 est.	$\rho_m - \rho_i$	PEFP (km)	D (Nm)	α (km)	M_0 ($N m^{-1}$)	M_{max} ($N m^{-1}$)	V_{max} ($N m^{-1}$)	V_0 (N/m)	Load Alps ($N m^{-1}$)
A	25	21.756	21.750	800	100	9.72×10^{22}	83.9	1×10^{16}	1.93×10^{17}	1.43×10^{13}	0.50×10^{13}	0.93×10^{13}
B	26	17.471	18.600	800	160	1.09×10^{23}	86.4	1×10^{16}	1.64×10^{17}	1.18×10^{13}	0.50×10^{13}	0.68×10^{13}
C	21	16.534	16.500	800	140	5.76×10^{22}	73.6	2.5×10^{16}	1.11×10^{17}	0.94×10^{13}	0.35×10^{13}	0.59×10^{13}
D	16	9.622	9.500	800	210	2.55×10^{22}	60.1	1×10^{16}	0.44×10^{17}	0.45×10^{13}	0.45×10^{13}	0.0×10^{13}
E	07	7.633	7.500	800	180	2.13×10^{21}	32.3	—	0.10×10^{17}	0.03×10^{13}	0.06×10^{13}	-0.03×10^{13}

W_0 est. (estimated) is the observed maximal depth of the European plate, taken from Gutscher (1995). $\rho_m - \rho_i$ is the density difference between mantle and inflill of the basin. PEFPP is the plate end free point, the position of the free end of the downflexing European plate in respect to the origin of the profile-lines. D is flexural rigidity and α the flexural parameter. M_{max} and V_{max} have been determined numerically, M_0 and V_0 are the applied values. The topographic load of the Alps has been determined by subtracting V_0 from V_{max} . Note decreasing deflection, EET and applied loads from A to E.

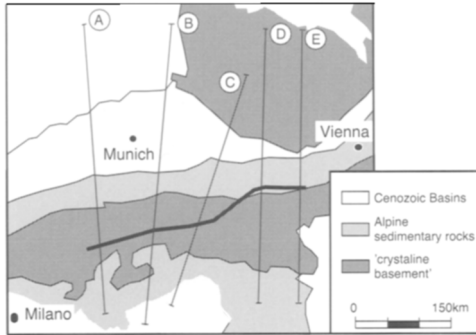


Fig. 8. Position of the PEFP along the profiles. The solid line connects the plate end free point of the five profiles. The increase in curvature of the plate (Fig. 10) towards the east causes: (1) narrowing of the basin to the east; (2) the lithospheric plate to continue less under the mountain chain to the east (that means less topographic load in the same direction).

to three times higher than the $3\text{--}4 \times 10^{12}\text{N m}^{-1}$ found by Gutscher (1995) leading to a conclusion that topographic loading is important.

Profile B (Fig. 7b). Like profile A, this profile is taken over the broad part of the GMB and yields results that are in the same order: an EET-value of 26 km and the downflexing European plate continues far under the topographic load (PEFP is 160 km, but the origin of this profile was placed slightly more southwards than that of profile A. Plotted in Fig. 10, the situation is very similar to profile A).

Profile C (Fig. 7c). This profile is in its northern part taken over the Bohemian Massif, along the southern border of this Massif, several basement faults (e.g. Donau- boundary trough) exist. The EET-value is slightly less than in profiles A and B: 21 km, the subsurface loads applied are in the same order or slightly lower. These values are required to model the tighter curvature of the European plate in this profile.

Profile D (Fig. 7d). The curvature of the deflection increases considerably when going from profile C to this profile. To reproduce this tighter curvature, the EET-value decreases to 16 km and the applied subsurface loads are closer to their maximum values than in the three above mentioned profiles. The free end of the plate in this profile is situated most basinward (see Fig. 8). Although the topography is relatively high, only small part of it is on top of the plate acting as a topographic load. This means that the topographic load should not be large. When

decreasing the EET-value, the deflection can only be modelled when applying subsurface loads that are in the same order as the ones we used before. As a consequence, the strength of the plate would be exceeded even more. Upon decreasing the subsurface loads, it is impossible to obtain a good fit to the deflection.

Profile E (Fig. 7e). This profile shows a very particular setting, with the rheologically strong Bohemian Massif very close to the frontal thrusts of the Alps, narrowing the basin extremely (only some 15 km). A compilation of several seismic lines by Tari (1996) and Wessely (1987) suggest that the European plate continues under the Danube Basin in Hungary. A complete deep seismic line, however, does not exist in the part of Austria where profile E runs. Moreover, the depth quality of the several smaller lines is poor (Tari 1996). The continuation of the plate has been altered by the several (17 Ma and less important 10 Ma) stretching events in the Styrian–Vienna Basin area with stretching factors of 1.3–1.6 (see Sachsenhofer *et al.* 1997 and cross section Tari 1996). The topographic load is small due to less high topography (see Fig. 9) and only little continuation under the Alpine chain of the downgoing plate, but the observed curvature of the plate is tight. These boundary conditions yield as a result a very weak plate with an EET-value of only 7 km. Because topographic loading is not very important, subsurface loads need to be applied. Due to the considerable weakness of the plate, the applied values for the subsurface loads exceed, however, the maximum applicable values. This would lead to breaking up or plastic deformation of the plate. The resultant zero value of the topographic loading by the Alpine chain (see Table 4) might be explained by this process.

A larger density contrast between mantle and infill is improving the analytical results (the flexural parameter 1 decreases with increasing density contrast, see equation 8 in Appendix. Therefore M_{\max} and V_o increase, see equations 6 and 7, Appendix, respectively). However, because the infill is less dense and the same deflection is being modelled, the EET-values will have to be decreased to obtain the same fit. This will in turn decrease the M_{\max} and V_o . These two counter-active processes determine very well a small range of solutions.

Lateral variations in EET

The EET-values for all of the profiles are small (26–7 km) and follow more or less the depth of the base of the mechanical crust, corresponding

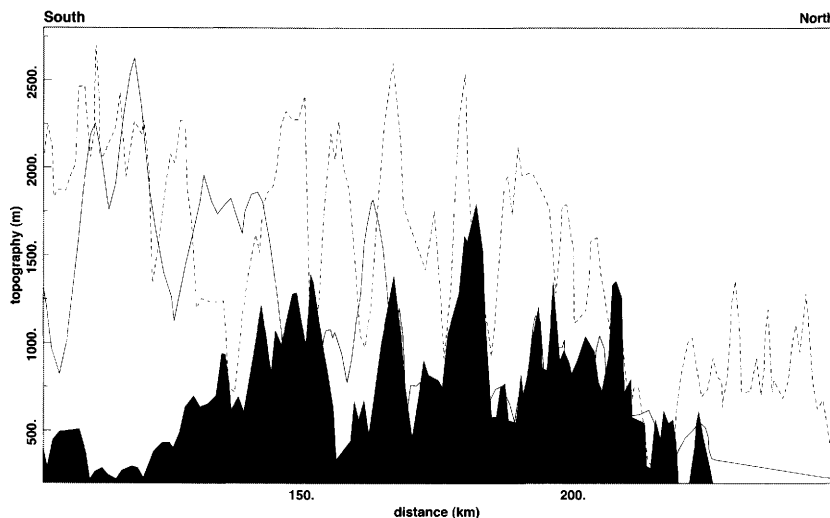


Fig. 9. Topographic load on profile lines B (dashed line), D (solid line) and E (black infill). Note significantly higher topography and thus larger topographic load for profile B.

with the 300–400°C isotherm (Burov & Diament 1995), pointing to crustal decoupling. The strength of the lithosphere is not very large due to pre-Alpine, Mesozoic stretching phases (see Fig. 5) and even more reduced (20–30%) by the plate boundary forces (Burov & Diament 1995). For profiles C, D and E strength most likely is even more reduced due to NW–SE-directed basement faults, that controlled sedimentation of Molasse sediments as well (e.g. Landshut–Neuöttinger zone, Donau-border fault). The lateral narrowing of the NAFB can not be explained by destruction of part of the originally full basin extent due to the Late Cenozoic uplift only. The curvature of the deflection (see Fig. 10) increases strongly from profile B to C and D, causing the broad part in the GMB to narrow laterally towards the AMB where the Bohemian Massif is as close as 15 km to the Alpine thrust sheets. The relatively rigid and strong Bohemian Massif might have squeezed the foreland basin when the Alpine front approached. The increase in curvature is explained by a decrease of the EET-values from 26 km to only 7 km (from respectively profile B to E). More to the east, where the NAFB continues into the northern Carpathian foreland basin, the basin widens again and EET estimates from forward modelling yield slightly higher values (in the order of 12 km near Brno, Zoete-meijer pers. comm.). Therefore, the results of our study appear to be in agreement with the observations and are compatible with the overall tectonic setting.

An equally good fit might be obtained with a situation in which the EET value decreases in the most flexed area. The calculation of the maximum applicable subsurface loads becomes very complex in that case, moreover because deformation might be localised in the weaker parts of the plate. Therefore we used a constant value for the EET in our modelling.

The position of the free end of the plate (PEFP) along the profiles (see Fig. 8) corresponds closely to the tightness of the deflection of the downgoing plate (the steeper the dip, the less easy to continue horizontally far under the mountain chain) and thus to the EET-value. In profile A and B, the European plate dips gently under the loading African plate and continues south to approximately the position of the Insubric Line. To the east in profiles C, D and E, the dip of the plate is much larger and, therefore, the plate does not continue very far southwards under the collision belt. In this way only a small part of the Alps is acting as a topographic load in the latter profiles. The cross section compiled by Tari (1994, 1996), suggests that the European Plate continues far south under the Danube Basin. Most likely this continuation is not formed by the entire plate, but only the upper crust whereas the lower crust and mantle part might have decoupled and broken down. This option, that seems in favour with rheological strength calculations showing a weak mantle and lower crust in this area (Lankreijer 1998), can not be modelled with the used flexural modelling approach. In this way, the subduction

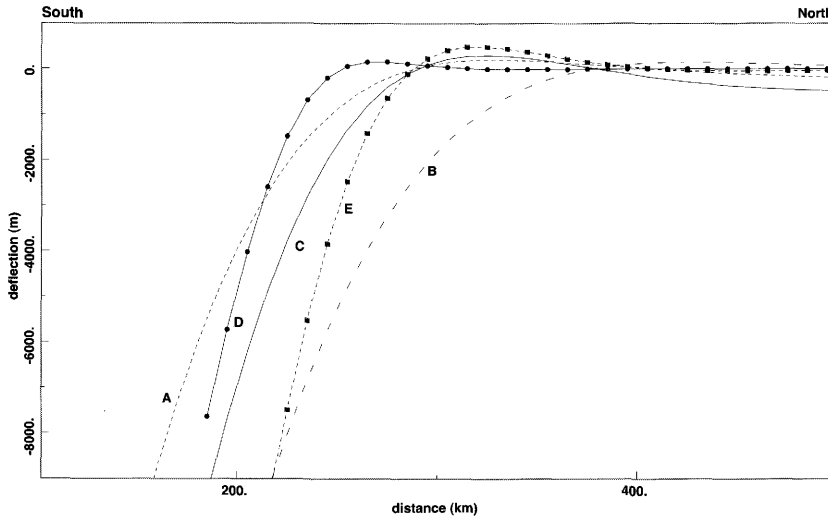


Fig. 10. Best fit to the restored deflection along all of the profiles compared. Closely dashed line: profile A, loosely dashed line: profile B, solid line: profile C, solid line with dots: profile D, dashed line with squares: profile E. Curvature increases progressively from profile A to E.

related Karpatian–Badenian volcanism observed in the southern Styrian Basin could be explained by downgoing and melting of the upper crust. The origin of this volcanism is however still a matter of debate (Sachsenhofer *et al.* 1997).

Origin of the Cenozoic uplift/unflexing'

The 'unflexing' following the flexural phase (see Fig. 11 for a schematic illustration) is a process that is observed clearly in the NAFB (and other foreland basins as well, e.g. Desegaulx *et al.* 1991; Kruse & Royden 1994). Its origin, however, is far from clear. Royden (1993) concluded that subsurface loads actually cause uplift of the foreland basement beneath the foredeep basins on both sides of the Alps and only cause subsidence beneath the internal parts of the thrust belt. Geodetic observations however demonstrate that recent uplift-values under the outer parts of the basin are in the same order ($0.5\text{--}1.2\text{ mm a}^{-1}$) as close to the frontal thrusts or in the internal parts of the Alpine chain (Jouanne *et al.* 1995), interpreted as the result of ongoing deformation along low-angle basement faults. This at least shows that the Late Cenozoic uplift, that is observed in all of the Alpine chain as well as in its foreland basins, is not the result of the action of subsurface loads only.

A possible cause for the uplift would be recovery of strength. As long as orogeny continues, the strength of the lithosphere

underlying the orogenic belt decreases; plate unloading results in an increase of the lithospheric strength (Burov & Diament 1995). Unloading of the plate by erosion or tectonic removal of the mountain load, would lead to major uplift in the orogeny, but only minor uplift in the foreland. Recovery of strength by the European plate would lead to unflexure. The term unflexure implies the decrease in amplitude of a bended plate, at least partly, back to its original unflexed shape. In other words, it would lead to subsidence of the bulge and uplift of the Alpine chain. This uplift pattern is not observed in the NAFB and therefore, unflexing can not be the governing process causing the uplift.

This uplift is used by Lyon-Caen & Molnar (1989) as an argument for an Alpine parallel upwelling theory. They point out that a possible cause for this process might be a diminution or termination of downwelling of mantle material beneath the Alps, due to breaking up of the downgoing plate ('slab detachment') and decrease of the north-south component of the convergence rate between the African and European plate. The calculated anomalies and the restored pre-uplift anomalies show remarkably equal trends (see Fig. 12 a b). However, the calculated anomaly is $+80\text{ mGal}$ when compared with the restored one, which is supposed to be a large negative anomaly due to the downward flexure of the plate to produce the sedimentary basin. To fit the calculations to the observations, a large scale lithospheric process that affected all

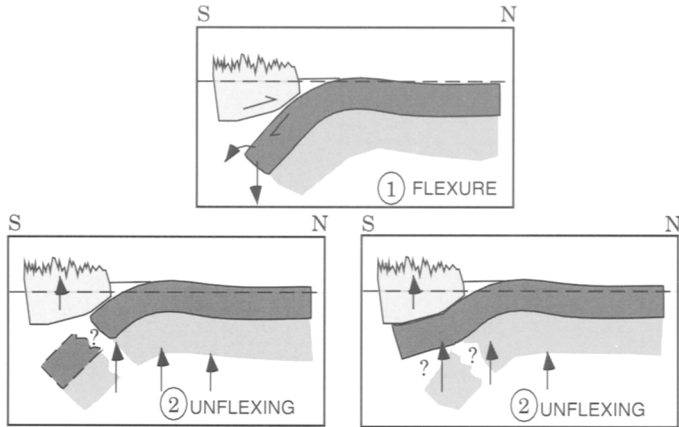


Fig. 11. Cartoon illustrating the two-phase evolution of the NAFB: (1) flexural response of the mechanically weak European lithosphere on loading by the overthrusting African plate creates a foreland basin; (2) two scenarios for Unflexing, Late Cenozoic uplift due to tectonic processes operating in the Alpine region. The thrust-belt and its foreland are uplifted several hundreds of meters in a post-molasse stage. Dashed line denotes approximately sea level.

of the Alpine region is needed. The problems encountered in modelling the profiles D and E, where the applied conditions in spite of all efforts still exceed the strength of the plate, would lead to breaking up of part of the plate. In this way, this study suggests decoupling of the upper crust, with breaking off of the lower crust and mantle, thus enabling the late Cenozoic uplift.

Thick plate versus thin plate models—a discussion

Studies concerning the Northern Alpine Foreland Basin have yielded a wide range of EET-values, from 7.5 km (Sinclair *et al.* 1991) to 53 km (Gutscher 1995). Karner & Watts (1983) estimated the EET of the European foreland to be between 25 to 50 km, but to obtain a good fit of the elastic model predictions to both flexure and gravity anomaly, additional subsurface loads (V_0 ranging from $1.4 \times 10^{14} \text{ N m}^{-1}$) were adopted. The nature and origin of these subsurface loads are not known, but their existence seems to be justified by the fact that surface loads and crustal blocks alone can not produce the observed flexure, the so called model of 'insufficient topography', observed in the Apennines as well (Royden 1993). The contribution of the subsurface loads to both observed gravity and amplitude and wavelength of the flexural basin is substantial. The role of the surface load becomes increasingly important, however, as the strength of the lithosphere decreases. The strength of the

European lithosphere under the Alps is small, due to pre-orogenic stretching and crustal shortening (Lyon-Caen & Molnar 1989), so loading by the Alpine orogenic belt should be of major importance in this case. Royden (1993) favours topographic loading as the cause of most of the deflection, with only a minor contribution of the subsurface loads in flexure under the Alps. However, in the sections presented in Royden (1993) both a too large M_0 ($2.5\text{--}9.0 \times 10^{17} \text{ N}$) and V_0 ($0.9\text{--}3.6 \times 10^{12} \text{ N m}^{-1}$) are applied at the free end of the plate.

Lyon-Caen & Molnar (1989) pointed out that the elastic model can not be adequate if such a set of parameters is required to account for the observed gravity gradient over the Molasse Basin and the Alpine Chain, and reject the use of unknown subsurface loads. Lyon-Caen & Molnar (1989) argue that the dynamic processes that created the deflection and built the Alpine Chain are no longer active. Our study supports the latter idea with the elastic plate model itself not being able to model the observed deflection of the European plate under the NAFB. Adopting additional subsurface loads appears to be justified as long as their limits are taken into account using the analytical equations (given in the Appendix).

Jin (1995) numerically estimated the wavelength of the lithosphere and in this way determined a flexural rigidity that corresponds to an EET value of 48 km for the underlying the German Molasse Basin. Since the shape of the deflection has been altered significantly due to

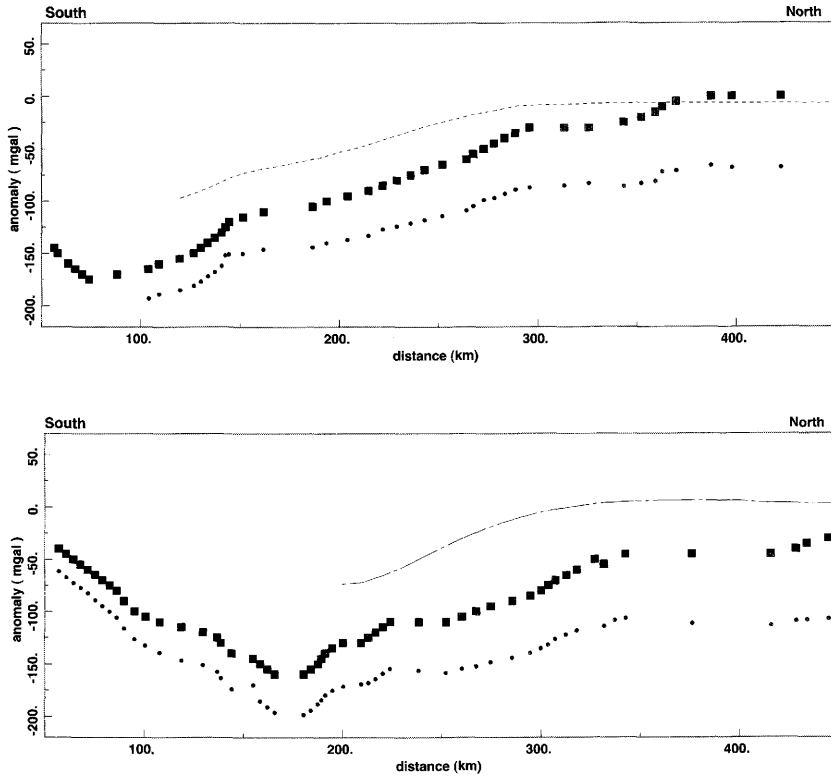


Fig. 12. Observed (squares), restored (dots) and calculated (dashed line) anomaly patterns along respectively profile A and C. The restored and calculated anomalies show remarkably equal trends but are offset c.80 mGal (profile A) and c.120 mGal (profile C).

the later uplift, this estimate seems not to be justified.

Recently Gutscher (1995) tried to explain the presently observed anomalously high topography in the NAFB by deflecting an elastic plate with large EET-values (53 km in the east to 34 km in the west over the Rhine Graben) loaded by the surface load of the Alps ($1\text{--}3 \times 10^{12} \text{N m}^{-1}$) and additional V_0 ($2\text{--}5 \times 10^{13} \text{N m}^{-1}$). EET-values of this order seem in favor of crustal coupling (Burov & Diament 1995) strengthening the lithospheric plate considerably. In this way the large applied loads (surface and subsurface) can be supported by the lithosphere, creating a tight curvature and obtaining a bulge of 1000–1500 m. This, however is in contradiction with the geological observations: Upper Marine Molasse sediments of Mid-Miocene age, were sedimented below sea level (which differed approximately +0–100 m from the present sea level, Lemcke 1988; Jin 1995), but are nowadays exposed at levels up to 850 m above sea-level (Lemcke 1988, fig. 55). If such a flexural bulge

would have been present before sedimentation of the Molasse as proposed by Gutscher (1995), the Molasse sediments (*s.s.*) should be onlapping onto the bulge, instead of being exposed on top of its crest. The last major loading event in this region is the emplacement of the Helvetic Nappes from Eocene to Miocene (50–10 Ma). The thrust nappes in this area reached their present-day position at about the Egerian–Eggenburgian boundary (Early Miocene c.20–18 Ma, Genser *et al.* 1997), so no significant shift or uplift of the bulge due to loading is to be expected after Miocene. The major shallowing upwards cycle of Upper Marine Molasse to Upper Freshwater Molasse was deposited in the flexural depression and only uplifted in a post-molasse stage (Lemcke 1988). Moreover, the EET values adopted by Gutscher (1995) and Jin (1995) are incompatible with estimates based on synthetic rheological profiles (Cloetingh & Burov 1996) and to the notion that the European plate was a very weak plate at the onset of loading due to Mesozoic extension (see Fig. 5).

This is another argument that supports the model presented here.

Conclusions

The deflection of the European plate underlying the NAFB due to overthrusting of the African plate, can be modelled in terms of an elastic plate model loaded by the Alpine thrust belt and limited subsurface loads with superposition of a Late Cenozoic (post flexural deflection) uplift of several hundreds of metres (see Fig. 11). Therefore, foreland basins that experienced post-molasse uplift, should not be studied as the effect of a flexural stage only, to avoid overestimates of subsurface loads and/or EET values.

The EET values that result from this study range from 7 to 26 km for the several profiles. These values are in accordance with models of a depth dependent continental rheology (e.g. Cloetingh & Banda 1992; Cloetingh & Burov 1996; Okaya *et al.* 1996) that predict for the foreland basins of the Alps a mechanically very weak lithosphere with characteristic EET-values of 10–25 km, as inferred for other parts of the European Alpine system (e.g. Zoetemeijer *et al.* 1990; Burov and Diament 1995; Cloetingh & Burov 1996; Okaya *et al.* 1996). The values adopted for the flexural parameters that deflect the lithosphere (V_o , M_o and EET) in most of the previous studies (e.g. Royden 1993) would exceed the elastic strength of the mechanically weak lithosphere that is present under the NAFB and thus cause plastic deformation or breaking-up. All these studies attempted to model the presently observed flexure as the result of one single flexural process. However, it is more likely that the present configuration of the NAFB is the result of (1) a flexural process forming the foreland basin due to loading by the African plate with superimposed (2) a subsequent ‘unflexing’ stage expressed in significant post-Molasse (Late Cenozoic) uplift of the whole region. This uplift might be caused by breaking up or delamination of part of the European crust.

We would like to thank J. Genser and R. Moeys for their contributions to the early phase of this work, H. P. Luterbacher and J. Zweigel for discussion and data. R. Zoetemeijer and A. Lankreijer are thanked for helpful discussions and comments. This work was funded by the IBS Project. Contribution 970124 of the Netherlands Research School of Sedimentary Geology.

Appendix 1

Analytical determination of the maximum values for the subsurface loads

Maximum bending moment

For a broken plate scenario, the maximum bending moment that can be applied to the lithospheric plate under consideration can be determined (see for a more detailed derivation Turcotte & Schubert 1982).

The bending moment of an elastic plate is given by:

$$M(x) = -D \frac{d^2w}{dx^2} \quad (\text{Eq. 2})$$

where D is the flexural rigidity of the considered plate.

The maximal applicable bending moment will reach its maximum when either D (large EET value) or $w''(x)$ is maximal and thus $w'''(x) = 0$. This is solved differentiating three times the general equation of the deflection of a broken plate:

$$w'''(x) = \frac{2w_0}{\alpha^3} e^{-\frac{x}{\alpha}} (\cos \frac{x}{\alpha} - \sin \frac{x}{\alpha}) = 0 \quad (\text{Eq. 3})$$

so that the location where the bending moment is maximal becomes:

$$x_{\max} = \frac{\alpha}{\tan(1)} = \frac{\pi}{4} \alpha. \quad (\text{Eq. 4})$$

From eq.1 and realizing:

$$w''(x) = \frac{2w_0}{\alpha^2} e^{-\frac{x}{\alpha}} \sin \frac{x}{\alpha} \quad (\text{Eq. 5})$$

the maximum bending moment at x_{\max} is:

$$M_{\max} = \frac{-2Dw_0}{\alpha^2} e^{-\frac{\pi}{4}} \sin \frac{\pi}{4} \quad (\text{Eq. 6})$$

Vertical Force

Like the bending moment M_o , V_o can be determined numerically:

$$V_o = \frac{4DW_0}{\alpha^3}. \quad (\text{Eq. 7})$$

This V_o -value is the combination of topographic load and an additional vertical force at the free end of the plate (plate end free point, PEFP).

The dependency of the flexural parameter α on the density contrast of infill and mantle material is given by:

$$\alpha = \left[\frac{4D}{g(\rho_m - \rho_i)} \right]^{\frac{1}{4}}. \quad (\text{Eq. 8})$$

References

- ALLEN, P. A., CRAMPTON, S. L. & SINCLAIR, H. D. 1991. The inception and early evolution of the North Alpine Foreland Basin, Switzerland. *Basin Research*, **3**, 143–163.

- BACHMANN, G. H. & MÜLLER, M. 1992. Sedimentary and structural evolution of the German Molasse Basin. *Ecolage Geologicae Helvetiae*, **85**, 519–530.
- , — & WEGGEN, K. 1987. Evolution of the Molasse Basin (Germany, Switzerland). *Tectonophysics*, **137**, 77–92.
- BODINE, J. H., STECKLER, M. S. & WATTS, A. B. 1981. Observations of flexure and the rheology of the oceanic lithosphere. *Journal of Geophysical Research*, **86**, 3695–3707.
- BUROV, E. B. & DIAMENT, M. 1995. The effective elastic thickness (T_e) of continental lithosphere: What does it really mean? *Journal of Geophysical Research*, **100**, 3905–3927.
- CLOETINGH, S. & BANDA, E. 1992. Mechanical structure of Europe's lithosphere. In: BLUNDELL, D., FREEMAN, R. & MUELLER, S. (eds) *A continent revealed, the European Geotraverse*, 80–91.
- & BUROV, E. B. 1996. Thermomechanical structure of European continental lithosphere: constraints from rheological profiles and EET estimates. *Geophysical Journal International*, **124**, 695–723.
- DESEGAULX, P., KOOI, H. & CLOETINGH, S. 1991. Consequences of foreland basin development on thinned continental lithosphere: application to the Aquitaine basin (SW France). *Earth and Planetary Science Letters*, **106**, 116–132.
- GENSER, J., VAN WEES, J. D., CLOETINGH, S. & NEUBAUER, F. 1996. Eastern Alpine tectono-metamorphic evolution; Constraints from two-dimensional P-T-t modelling. *Tectonics*, **15**, 584–604.
- GUTSCHER, M. A. 1995. Crustal structure and dynamics in the Rhine Graben and the Alpine foreland. *Geophysical Journal International*, **122**, 617–636.
- JIN, J. 1995. *Dynamic stratigraphy analysis and modelling in the south-eastern German Molasse Basin*. Tübinger Geowissenschaftliche Arbeiten, **A24**.
- JOUANNE, F., MENARD, G. & DARMENDRAIL, X. 1995. Present-day vertical displacements in the north-western Alps and southern Jura Mountains: Data from leveling comparisons. *Tectonics*, **14**, 606–616.
- KARNER, G. D. & WATTS, A. B. 1983. Gravity anomalies and flexure of the lithosphere at mountain ranges. *Journal of Geophysical Research*, **88**, B12, 10449–10477.
- KRUSE, S. E. & ROYDEN, L. H. 1994. Bending and unbending of an elastic lithosphere: the Cenozoic history of the Apennine and Dinaride foredeep basins. *Tectonophysics*, **13**, 278–302.
- LANKREIJER, A. 1998. *Rheology and basement control on extensional basin evolution in Central and Eastern Europe: Variscan and Alpine-Carpathian-Pannonian tectonics*. PhD thesis, Vrije Universiteit, Amsterdam.
- LEMCKE, K. 1972. Die Lagerung der jüngsten Molasse in nördlichen Alpenvorland. *Bulletin der Vereinigung Schweizerischen Petroleum Geologen und -Ingenieurs*, **39**, 29–41.
- 1988. *Geologie von Bayern I. Das bayerische Alpenvorland vor der Eiszeit*. E. Schweizerbartische Verlagsbuchhandlung, Stuttgart.
- LYON-CAEN, H. & MOLNAR, P. 1989. Constraints on the deep structure and dynamic processes beneath the Alps and adjacent regions from an analysis of gravity anomalies. *Geophysical Journal International*, **99**, 19–32.
- MATENCO, L., ZOETEMEIJER, R., CLOETINGH, S. & DINU, C. 1997. Lateral variations in the mechanical properties of the Romanian external Carpathians: inferences of flexure- and gravity modelling. *Tectonophysics*, **28**, 147–166.
- MILLAN, H., DEN BEZEMER, T., VERGES, J., MARZO, M., MUNOZ, J. A., ROCA, E., CIRES, J., ZOETEMEIJER, R. & CLOETINGH, S. 1995. Paleo-elevation and effective elastic thickness evolution of mountain ranges: inferences from flexural modelling in the Eastern Pyrenees and Ebro Basin. *Marine and Petroleum Geology*, **12**, 917–928.
- NACHTMANN, W. & WAGNER, L. 1986. Mesozoic and Early Tertiary evolution of the Alpine foreland in Upper Austria and Salzburg, Austria. *Tectonophysics*, **137**, 61–76.
- OKAYA, N., CLOETINGH, S. & MÜLLER, S. T. 1996. A lithospheric cross-section through the Swiss Alps (part II): constraints on the mechanical structure in continent-continent collision zones. *Geophysical Journal International*, **127**, 399–414.
- PEPER, T., VAN BALEN, R. & CLOETINGH, S. 1994. Implications of orogeny, intraplate stress variations and eustatic sealevel change for foreland basin stratigraphy – inferences from numerical modelling. In: DOROBOK, S. & ROSS, G. (eds) *Stratigraphy and foreland basins*. SEPM Special Publications, **52**, 5–35.
- ROYDEN, L. H., 1993. The tectonic expression of slab pull at continental convergent boundaries. *Tectonics*, **12**, 303–335.
- & KARNER, G. D. 1984. Flexure of the continental lithosphere beneath the Apennine and Carpathian foredeep basins: evidence for insufficient topography. *American Association of Petroleum Geologists Bulletin*, **68**, 704–712.
- SACHSENHOFER, R. F., LANKREIJER, A., CLOETINGH, S. & EBNER, F. 1997. Subsidence analysis and quantitative basin modelling in the Styrian Basin (Pannonian Basin system, Austria). *Tectonophysics*, **272**, 175–196.
- SINCLAIR, H. D., COAKLEY, B. J., ALLEN, P. A. AND WATTS, A. B. 1991. Simulation of foreland basin stratigraphy using a diffusion model of mountain belt uplift and erosion: an example of the central Alps, Switzerland. *Tectonics*, **10**, 599–620.
- STOCKMAL, G. S., BEAUMONT, C. & BOUTILIER, R. 1987. Geodynamic models of convergent margin tectonics: transition from rifted margin to overthrust belt and consequences for foreland basin development. *American Association of Petroleum Geologists Bulletin*, **70**, 2, 181–190.
- TARI, G. C. 1994. *Alpine tectonics of the Pannonian Basin*. PhD thesis, Rice University, Houston, Texas.
- 1996. Extreme crustal extension in the Raba River extensional corridor (Austria/Hungary). *Mitteilungen der Gesellschaft der Geologie und Bergbaustudenten in Österreich*, **41**, 1–17.
- TRÜMPY, R. (ed.) 1980. *Geology of Switzerland, a guide book*. Wepf, Basel.

- TURCOTTE, D. L. & SCHUBERT, G. 1982. *Geodynamics*. John Wiley, New York.
- WATTS, A. B. 1992. The effective elastic thickness of the lithosphere and the evolution of foreland basins. *Basin Research*, **4**, 169–178.
- WESSELY, G. 1987. Mesozoic and Tertiary evolution of the Alpine-Carpathian foreland in eastern Austria. *Tectonophysics*, **137**, 45–59.
- ZOETEMEIJER, R. 1993. *Tectonic modelling of foreland basins, thin skinned thrusting, syntectonic sedimentation and lithospheric flexure*. Ph.D. Thesis, Vrije Universiteit Amsterdam.
- , DESEGALX, P., CLOETINGH, S., ROURE, F. & MORETTI, I. 1990. Lithospheric dynamics and tectonic-stratigraphic evolution of the Ebro-Basin. *Journal of Geophysical Research*, **95**, 2701–2711.